MINISTERE DU BUDGET

direction générale
des douanes
et droits indirects

" Copie pour information "

Sous direction
des affaires juridiques
et contentieuses

PROCES VERBAL

DE CESSION

Bureau D/2

24 JUIN 1993

№ 01652

En vertu des dispositions de l'article 390 § 1 du code des douanes et de l'article 6 § 3-c de l'arrêté du 26 septembre 1949, les marchandises suivantes, abandonnées après transaction au profit de l'administration des douanes sont remises à titre gracieux à Monsieur le Directeur des Musées de France:

- deux défenses d'éléphant entières, non travaillées, de 140 cm de longueur et d'un poids respectif de 20 Kgs 200 et 20 Kgs 300,

- deux défenses d'éléphant de 73 et 78 cm, d'un poids total de 6 Kgs.

Paris, le
Le directeur général des
douanes et droits indirects,

Je soussigné, Monsieur Jacques SALLOIS, Directeur des Musées de France, reconnais avoir reçu les objets visés ci-dessus. Qui seront mis à l'inventaire des collections des musées de France

Paris, le
Le directeur des Musées de France,

S1 Figs.

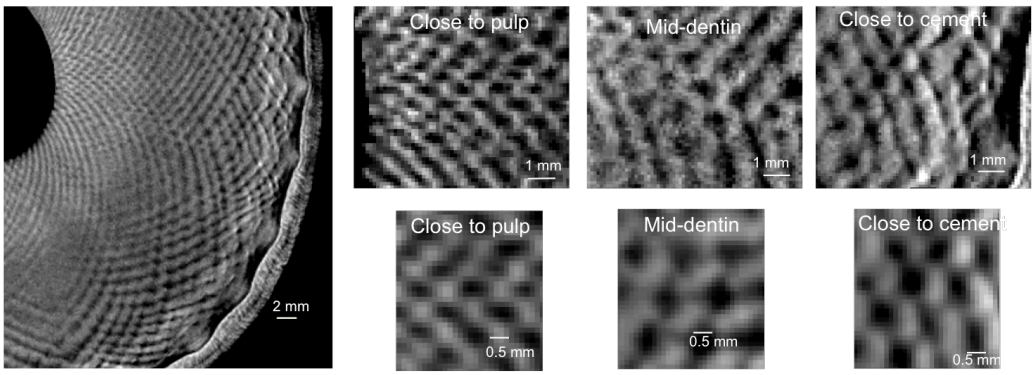

Figure A: Schreger pattern of the transverse plane difference in the rhomboids shape from cement to pulp. Close to the pulp the rhomboids are rectangles (0.2 x 0.5 mm^2) with their short dimension aligned along the pulp cavity, in the mid-dentin they have squared shape (0.5 x 0.5 mm^2) and close to the cement they are rectangles with their longest dimension along the

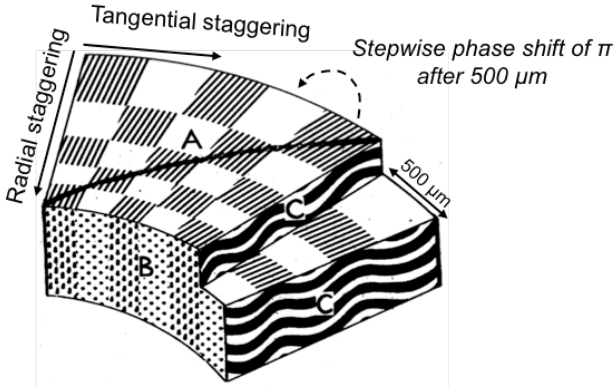

Figure B: Miles and White (1960) 3D model of the tubular microstructure with the radial and tangential staggering indicated and the phase shift of π after 500 µm

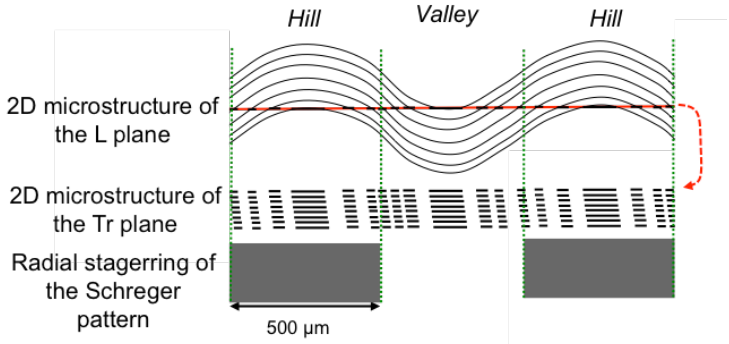

Figure C: Relation between the macroscopic Schreger pattern of the transverse plane and the tubular microstructure. According to Miles and White model, hills of the tubules correspond to the dark rhomboids of the Schreger pattern of the transverse plane, and valleys relate to the bright ones. Once sinusoidal tubules are cut perpendicular to their main axis, ie. in the transverse plane, the 2D microstructure results in an alternating regions of short and long lines. The 2D microstructure of the transverse plane is the same in dark and bright rhomboids according to Miles and White model.

S2 Figs. Average dot spacing and coordinates of tubule cross-sections of a tangential fractured section of elephant ivory and description of the modeling of the two cubes of straight tubules.

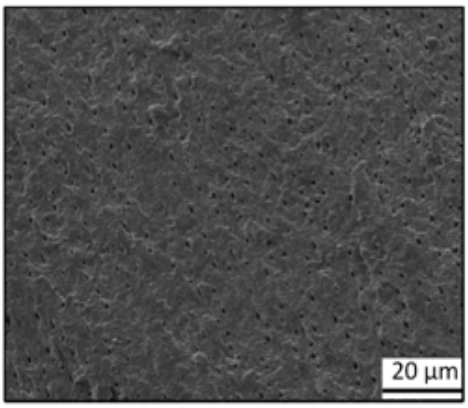

Figure A: SEM micrograph

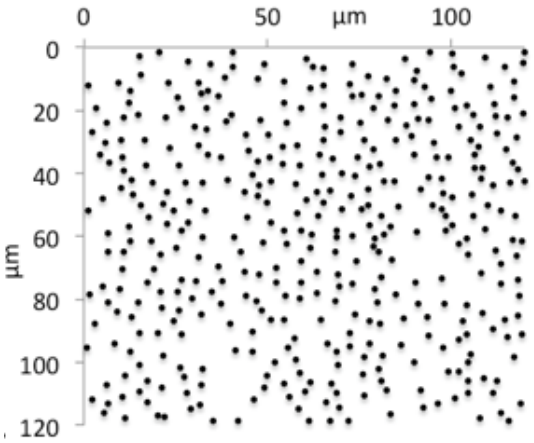

Figure B: Measured coordinates of every tubule cross-sections used to simulate the disordered cube.

S3 Fig. Virtual cut through an array of helical (or sinusoidal) tubules obtained through a series of successive cuts through individual tubules. Simulation of the intersection of many tubules with a cutting plane (i and vi) by calculation of the cross-sections in an iterative manner. The intersection of each individual tubule was calculated (ii-iii), and added to the intersection of the next tubule which is translated a known distance from the previous one (iv-v).

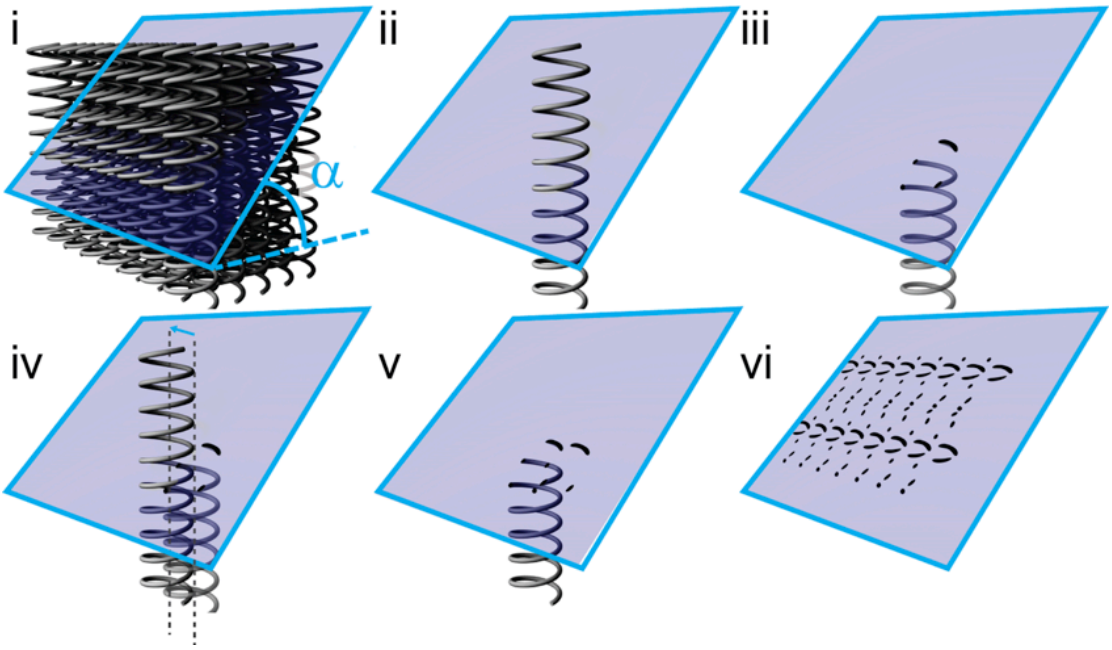

S4 Fig. Quantitative 2D elemental chemical maps of the transverse section of elephant ivory. 2D maps of 3 x 3 mm^2 of major elements of ivory (Ca and P), minor element (Mg) and traces (Na, S, Cl, K, Fe and Sr) obtained by Proton induced x-ray emission. Concentrations are expressed in wt.%.

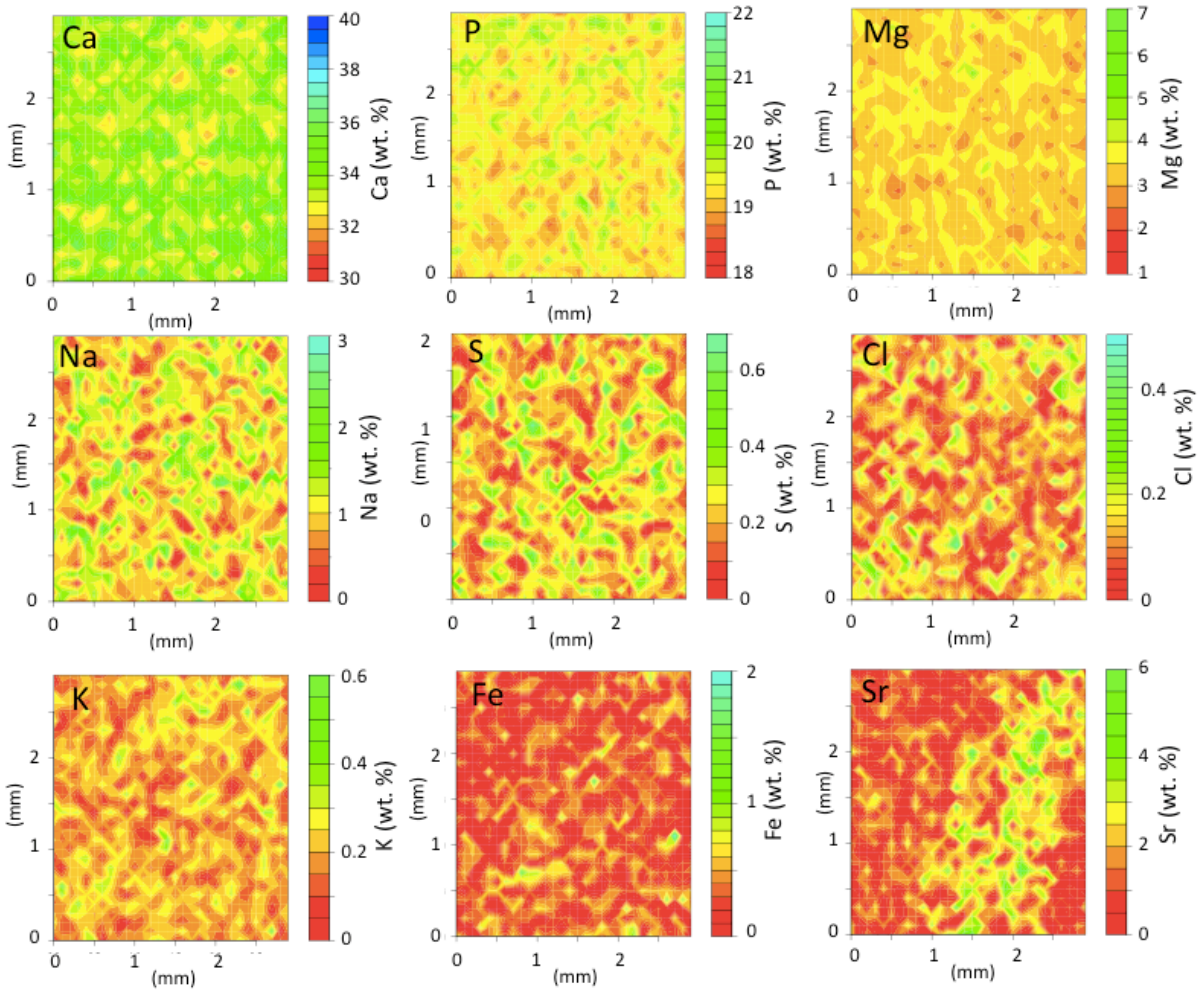

S5 Fig. Tubular sinusoidal trend of the transverse plane. Optical image of a thick polished section of the transverse plane located close to the cement. The mean amplitude of the tubular trend is 90 µm and its mean wavelength is 960 µm.

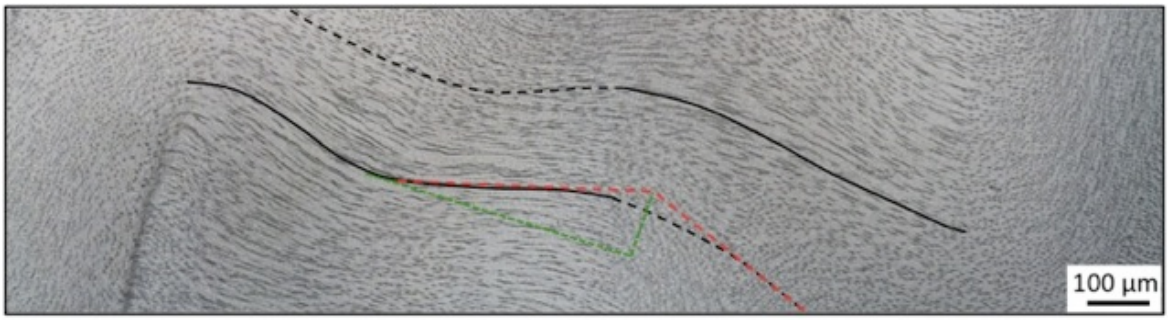

S6 Figs. Tubular cross-section arrangement and shape in the tangential plane.

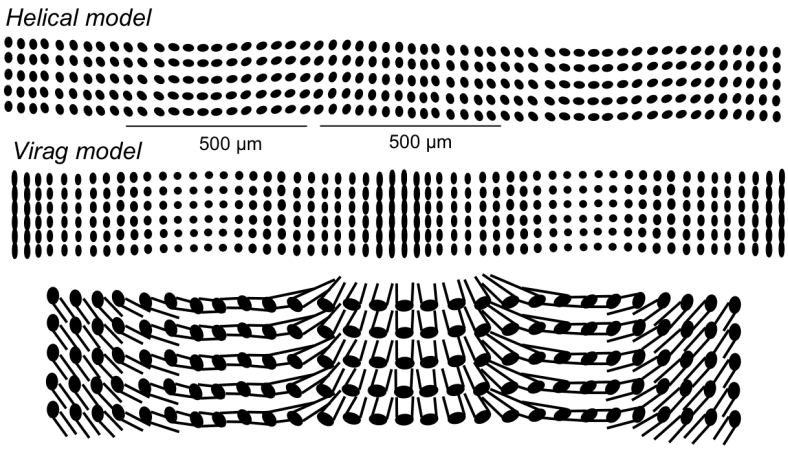

Figure A: Representation of our experimental observations and the one of Virag's model.

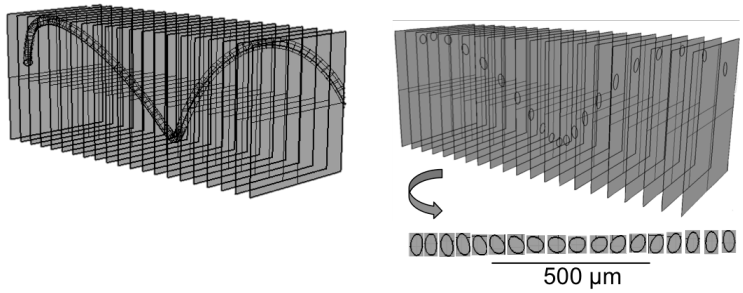

Figure B: Visualization of the shifted helical tubules behind the tubular cross-sections and simulated 2D planes of cut of the helix with the resulting cross-sections under every cutting plane. The obtained cross-sections have the same shape and orientation of the experimental data, suggesting that shifted helical tubules might likely be at the origin of the specific arrangement and shape of the tubular cross-sections observed in the tangential plane.

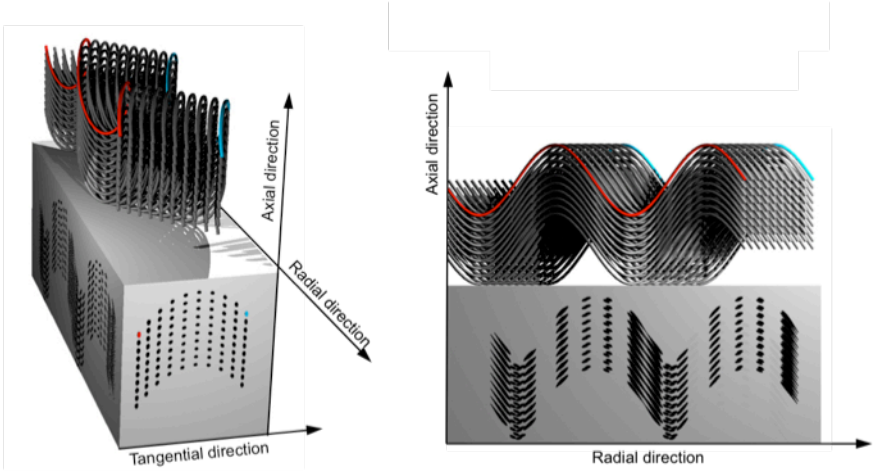

Figure C: 3D model of the distorted helical model showing the continuous phase shift of π after 1 mm in the tangential direction. The continuous phase shift is observed between the red and the turquoise tubule. The arrangement of the tubular cross-sections resulting from a longitudinal and tangential cut is also shown below the helical tubules.

S7 Figs. SR-µCT data of the 40 mm^3 volume with 1 µm resolution (voxel-size).

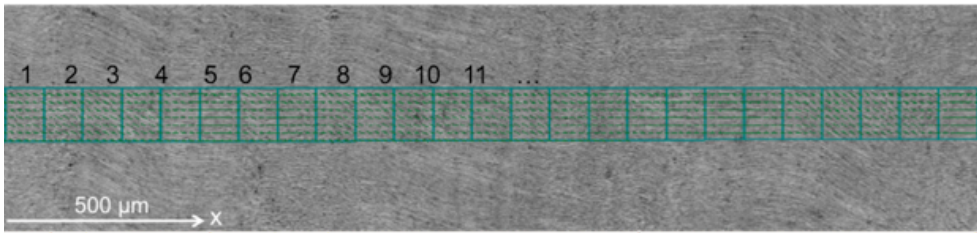

Figure A: 2D virtual section of the longitudinal plane where a sinusoidal trend for the tubule is observed, green squares indicate the segmentation of the 3D volume into 25 ROIs.

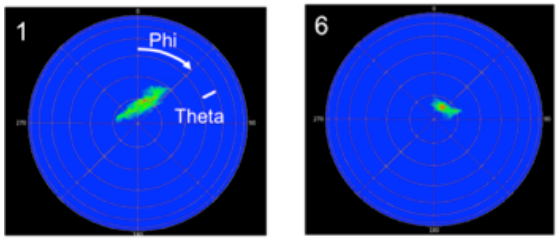

Figure B: determination of the average orientation of the main tubule axis for ROI number 1 and 6, Phi and Theta are represented for ROI 1 and 6 and measured for each ROI.

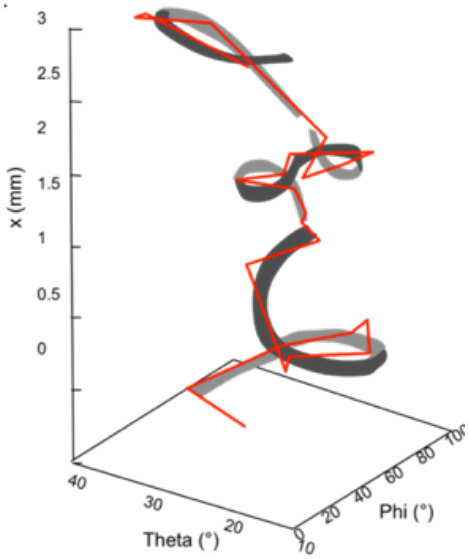

Figure C: 3D plot of Theta and Phi for each ROI, which allows us to evidence a helical shape of tubules.

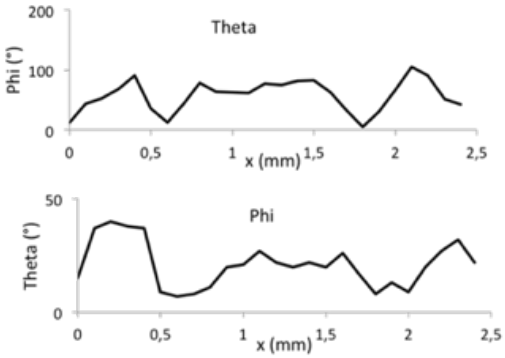

Figure D: 2D plot of Theta (x) and Phi (x) showing the approximated 1 mm pitch of the helix.

S8 Fig. SR-µCT data of the 5.10^{-4} mm^3 volume with 0.4 µm resolution (voxel-size). 2D SR-µCT images of the three planes, (xy), (xz) and (zy) and 3D visualization of the tubular network in the center.

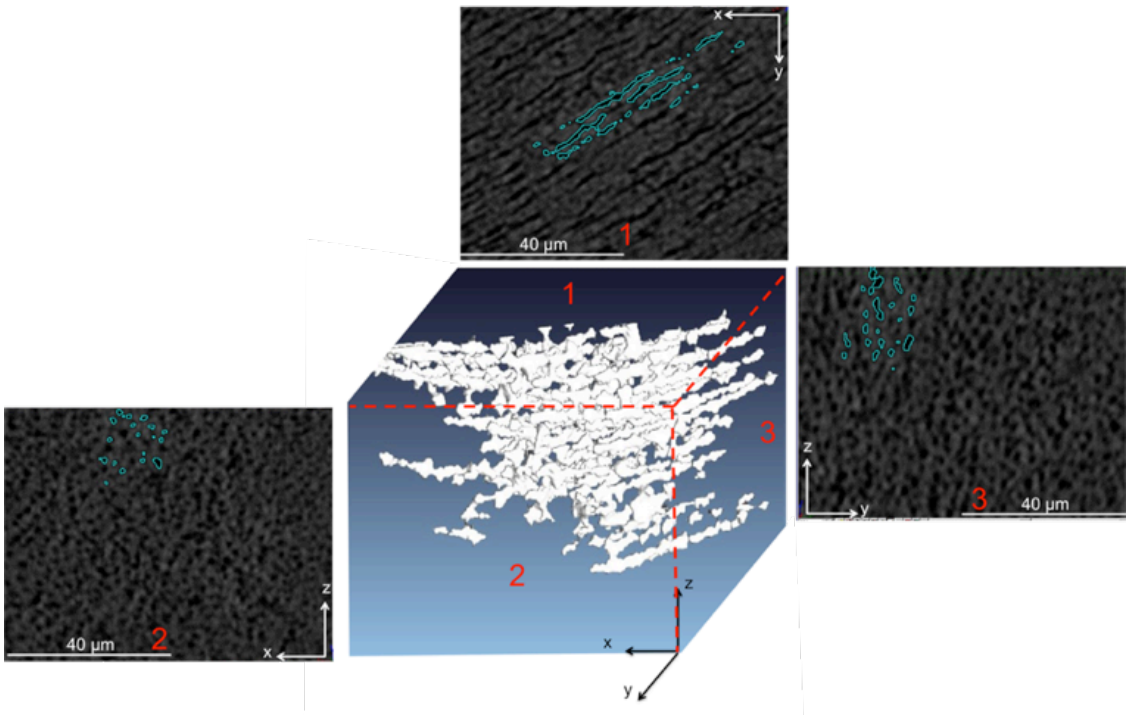

S9 Fig. Influence of light on the origin of the Schreger pattern. Two superimposed transverse sections of elephant ivory show the absence of mirror relation between the two sides in contact in terms of the colors of the Schreger pattern.

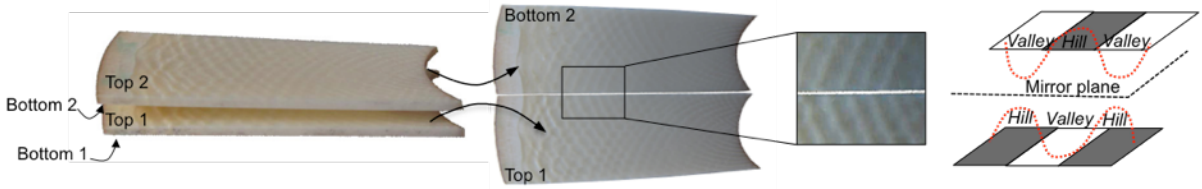

S1 Text.

Details on the modeling of the two cubes:

In order to simulate the role of the angle of the cutting plane α with respect to a rotation around an axis perpendicular to the tubules, two simple structures were simulated using the 3D software Rhinoceros (version 4 SR09) with the Grasshopper plugin (version 0-0-0061). The two structures contained linear tubules with a radius of 1 μm, one had a regular (square) array of tubule spaced 6 μm apart as determined from SEM measurements of the tangential plane, the other was an irregular array of tubules using the experimentally measured coordinates of tubules.

S2 Text. Modeling

In order to calculate the intersection of tubules with the three cutting planes (longitudinal, radial, and tangential) for the different 3D models of the tubular network of ivory, we simulated a variety of different structural models using the 3D software Rhinoceros (version 4 SR09) with the internal "Rhinoscript" scripting language.

The model of Miles and White assumed radially directed sinusoidal tubules (with an amplitude of 250 μm in the axial direction and a period of 1000 μm), spaced 6 μm apart in a square lattice (in the tangential plane). Every 500 μm in the tangential direction, the next group of tubules is phase shifted by an amount of π with respect to the previous group.

The Virag model also assumes sinusoidal tubules (with an amplitude of 300 μm in the axial direction and a period also of 1000 μm), however spaced 13 μm apart in a square lattice in the tangential plane. In contrast to the Miles and White model, this model includes, in addition to the stepwise phase shift of π every 500 μm in the tangential direction, a continuous phase shift in the tubules also in the tangential direction such that each sinusoid is shifted 13 μm in the radial direction with respect to its immediate neighbor in the tangential plane (i.e. a phase shift of 0.013*2π).

The helical model is based on the experimental results of this study, which suggests that the tubules are radially oriented helices that can be described by the equation $(a,t) = (230\sin(\frac{2\pi}{1000}r), 90\cos(\frac{2\pi}{1000}r))$ where a is the axial position of the tubule and t is the transverse position of the tubule with respect to the radially oriented helical axis, and r is the radial position. This model was tested for a regular square lattice of tubules in the tangential plane spaced 6 μm apart. Tubules were simulated 1) without phase shift, 2) with a gradual phase shift of 0.006*2π in the tangential direction and 3) a stepwise phase shift of π every 500 μm and a gradual phase shift of 0.006*2π in the tangential direction.

S10 Fig. highlights how a virtual cut through an array of helical (or sinusoidal) tubules can be obtained through a series of successive cuts through individual tubules, allowing for better memory usage in the computer. Simulation of the intersection of many tubules with a cutting plane (i and vi), which is computationally expensive to do in one step for biologically relevant tubule arrays, we calculated the cross-sections in an iterative manner. The intersection of each individual tubule was calculated (ii-iii), and added to the intersection of the next tubule which is translated a known distance from the previous one (iv-v).

S3 Text. Influence of light on the origin of the Schreger pattern.

Tubules are basic objects and have a mirror image whereas the colors of the Schreger pattern do not. The figure shows that when the adjacent faces of two serial transverse sections are compared (i.e. the top face of section 1 (Top 1) and the bottom face of section 2 (Bottom 2)), they are not mirror images of one another; rather, the bright bands of one section correspond to the dark bands of the other. We have demonstrated that lines and dots in transverse sections tend to be associated with bright and dark regions, respectively. However, here, hills and valleys of tubules, which are the same shape in transverse cross-section, are associated with different colors of the Schreger pattern in mirror image serial sections. This counterintuitive result was also implicitly shown in the model of Miles and White (1960), who drew a 3D scheme of a transverse ivory section, representing the radial staggering of the bright and dark rhomboids as corresponding respectively to the valleys and hills of sinusoidal tubules.

S4 Text. Detailed description of the 2D slices obtained by virtually cutting the 3D models

The transverse plane. The experimental transverse plane shows the structural staggered pattern with squared regions of dots and squared regions of lines of ~500 x 500 μm^2. Therefore, line areas (and dot areas) are observed every 1 mm in the radial direction and in the tangential direction (Fig 8a, transverse plane). Moreover, lines of maximum ~200 μm length are observed.
The simulated transverse plane of Miles&White model shows mainly dot features which progressively elongate to ~8 μm length in the radial direction (Fig 8b, transverse plane). No change is observed in the tangential direction. The 8 μm-long patterns occupy regions of ~120 μm size every 500 μm in the radial direction. By introducing a phase shift of $\pi/2$ instead of the one of π suggested by Miles&White model, an additional staggering in the tangential direction is created. Moreover, this modified version of Miles&White model shows longer lines up to ~30 μm.
The simulated transverse plane of Virag model shows also mainly dots (Fig 8b, transverse plane). They progressively elongate to maximum ~25 μm length in the radial direction. A continuous shift of the pattern is observed in the tangential direction and is due to the continuous phase shift of tubules. Diagonal line areas of ~100 μm size are present every ~500 μm.
The simulated transverse plane of the helical model without phase shift of the tubules shows alternated dot and line regions in the radial direction every 500 μm. Individual lines are ~30 μm and occupy regions of ~250 μm size (Fig 9a, transverse plane).
The simulated transverse plane of the helical model with a continuous phase shift of π after 1 mm shows diagonal areas of ~375 μm size every 750 μm containing lines of 45 μm length. Overlaps of helical tubules are observed every 750 μm (Fig 9b, transverse plane).
The simulated transverse plane of the helical model with a continuous phase shift of π after 1 mm and a stepwise phase shift of π after 0.5 mm shows too many overlaps to be considered for representing the experimental data (Fig 9c, transverse plane).

The longitudinal plane. The experimental longitudinal plane shows alternating vertical (in the axial direction) bands (~500 μm wide) of 100 μm-long line regions (lines inclined ~45° to the vertical of the section) and shorter line areas. Therefore, line regions (and dot regions) are observed every 1 mm in the radial direction. The juxtaposition of the long and short line regions present a sinusoidal trend in the radial direction (wavelength of 1 mm) (Fig 8a, longitudinal plane).
The simulated longitudinal planes of Miles&White and Virag models show complete sinusoids with a wavelength of 1 mm in the radial direction (Fig 8b 8c, longitudinal plane).
The arrangement of the tubular sections of the simulated longitudinal plane of the helical model without phase shift changes in the radial direction and stays the same in the tangential one (Fig 9a, longitudinal plane). It shows regions of dots and lines every ~300 μm with lines of 10 μm length.
The simulated longitudinal plane of the helical model with a continuous phase shift of π after 1 mm shows a very similar pattern to the previous model, with regions of dots and lines observed every ~750 μm. Vertical overlaps in the axial direction are present every 1 mm (Fig 10b, longitudinal plane).

The simulated transverse plane of the helical model with a continuous phase shift of π after 1 mm and a stepwise phase shift of π after 0.5 mm shows the same pattern as the previous model (Fig 10c, transverse plane).

The tangential plane. The experimental tangential plane shows a periodic change of orientation of the ellipsoidal cross-sections every 1 mm (Fig 8a, tangential plane).
The simulated tangential plane of Miles&White presents a regular array of circular tubular cross-sections. Modified Miles&White model shows in the tangential direction alternating circular and ellipsoid cross-section areas. Circular (and ellipsoid) areas are observed every 1 mm (Fig 8b, tangential plane).
The simulated tangential plane of Virag model shows periodic changes in the size of the cross-sections of the tubules in the tangential direction every ~500 μm (Fig 8b 8c, tangential plane), not every 1 mm as it was suggested in Virag (2012) (S6 Fig.).
The helical model without phase shift shows an array of regularly spaced ellipsoids and with the same orientation (Fig 9a, tangential plane).
The helical model with the continuous phase shift of π after 1 mm shows the periodic change of orientation of the ellipsoidal cross-sections every 1 mm. However, periodic overlaps every 1 mm are present in the simulated plane (Fig 9b, tangential plane).
The simulated tangential plane of the helical model with a continuous phase shift of π after 1 mm and a stepwise phase shift of π after 0.5 mm shows too many overlaps every 500 μm (Fig 9c, tangential plane).